DOI: 10.1002/chem.200600052

Resonance Structures of the Amide Bond: The Advantages of Planarity

Jon I. Mujika,[a] Jon M. Matxain,[b] Leif A. Eriksson,[b] and Xabier Lopez*[a]

Abstract: Delocalization indexes based on magnitudes derived from electron-pair densities are demonstrated to be useful indicators of electron resonance in amides. These indexes, based on the integration of the two-electron density matrix over the atomic basins defined through the zero-flux condition, have been calculated for a series of amides at the B3LYP/6-31+G* level of theory. These quantities, which can be viewed as a measure of the sharing of electrons between atoms, behave in concordance with the traditional resonance model, even though they are integrated in Bader atomic basins. Thus, the use of these quantities overcomes contradictory results from analyses of atomic charges, yet keeps the theoretical appeal of using nonarbitrary atomic partitions and unambiguously defined functions such as densities and pair densities. Moreover, for a large data set consisting of 24 amides plus their corresponding rotational transition states, a linear relation was found between the rotational barrier for the amide and the delocalization index between the nitrogen and oxygen atoms, indicating that this parameter can be used as an ideal physical-chemical indicator of the electron resonance in amides.

Keywords: amides · delocalization indexes · density functional calculations · resonance stabilization · rotational barrier

Introduction

The amide bond has attracted much attention because it is the essential structural motif of the protein backbone.[1,2] The amide bond has peculiar geometrical and energetic features, essential for its structural role as the building block of proteins. As the most characteristic properties, one can mention the planarity of the nitrogen atom, shorter C–N bond lengths than in amines, and larger C–O bond lengths than in aldehydes.[3–5] The amide bond is also very stable. This can be inferred from its rotational barrier around the C–N bond.[6–10] In addition, amide bonds show a characteristic stability towards nucleophilic attack.[11,12] Energetic stability is also important because it confers the required degree of stability and rigidity to the amide/peptide linkage necessary to act as the protein scaffold.

Not surprisingly, therefore, many theoretical studies have tried to explain these properties in terms of basic physical-chemical concepts. Traditionally, resonance theory and molecular orbital (MO) theory[13–16] have been used for this purpose. Early theories established, somewhat intuitively, that there is a resonance between the nitrogen lone pair (n_N) and the carbonyl π orbital (π_{CO}), which leads to a sp^2 hybridization of the nitrogen atom. In terms of standard resonance theory, the description of the electronic structure is accomplished through the introduction of two resonance structures (I and II in Scheme 1), with structure II leading to a partial double-bond character of the C–N bond, and therefore, its planarity and stability. In reality, the electrons in the double bonds are delocalized across the amide group, and the elec-

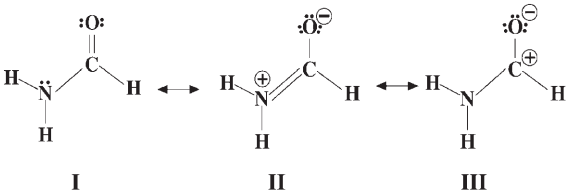

Scheme 1. Resonance structures used to describe the electronic structure in amides.

[a] J. I. Mujika, Prof. X. Lopez
Kimika Fakultatea
Euskal Herriko Unibertsitatea and
Donostia International Physics Center (DIPC)
P.K. 1072, 20080 Donostia, Euskadi (Spain)
Fax: (+34) 943-015-270
E-mail: xabier.lopez@ehu.es

[b] Dr. J. M. Matxain, Prof. L. A. Eriksson
Department of Natural Sciences and Örebro Life Sciences Center
Örebro University, 70182 Örebro (Sweden)

Supporting information for this article is available on the WWW under http://www.chemeurj.org/ or from the author. It contains a table displaying the ellipticity and electron density values at the C–N and C–O bond critical points for compounds **1**–**8** with R = H, methyl, and phenyl, and their rotational transition states.

 © 2006 Wiley-VCH Verlag GmbH & Co. KGaA, Weinheim

tronic structure is a hybrid of these two resonance contributions.

More recently, attempts have been made to quantify the resonance effect by using natural population analysis and natural resonance theory.[17] These studies support the traditional resonance model, showing that strong $n_N \rightarrow \pi^*_{C-O}$-type resonances lead to significant stabilization of the electronic structure in amides. Besides, analysis of the Mulliken atomic charges[18] as a function of C–N bond rotation also gives trends that are in agreement with the resonance model, predicting a transfer of electronic charge from nitrogen to oxygen as the C–N bond rotates. In addition, valence bond theory[19,20] has also lead to results in accordance with the resonance model.

However, the use of orbital and partitioning schemes such as Mulliken are not fully unambiguous criteria for ascertaining the nature of the electronic structure of molecules. Furthermore, an analysis based on localized orbitals could be far from adequate to describe electronic effects based on the delocalization of electron density among various nuclei.

Correspondingly, efforts have been made to use the electron density and its topological analysis, reliant on a nonarbitrarily modified physical observable, to characterize the nature of the electronic structure in amides.[21–26] However, analysis of the corresponding atomic charges, based on the integration of the electron density in the atomic volumes defined in the context of the Atoms-in-Molecules (AIM) theory,[27] led to a contradictory picture with respect to the resonance model and experimental estimates of electron density changes upon C–N rotation based on ^{13}C, ^{15}N, and ^{17}O NMR chemical shifts[28] and N1s and O1s core ionization energies.[29] Thus, a qualitatively different electronic charge transfer is predicted: a transfer of electronic charge from the nitrogen to the carbon atom, but with small changes within the oxygen atom. It has been argued[30] that the differences between the two analyses can be reconciled if one takes into account the high polarity of the C=O bond, thus observing the importance of resonant structure III.[25] Nevertheless, the controversy regarding the use of Bader atomic charges and their interpretation is not new,[31–33] and some authors[18] have even claimed that Bader atomic charges are not suitable for this kind of analysis.

In summary, questions remain as to the relation of the resonance in amides to a well-founded physical-chemical quantity that overcomes the limitations of the use of molecular orbitals and complements the useful analysis provided by orbital-based theories. In this vein, the present paper applies recently developed localization and delocalization indexes[34,35] to characterize the electron resonance in amides. These indexes have been successfully used to gain insight into the electronic structure of various molecules. They are based on the topological analysis of a well-defined unambiguous quantum object: the two-electron density matrix, which resembles the simultaneous probability density of finding two electrons at two points in space. Indexes derived from the two-particle density matrix are integrated over atoms following Bader's criteria for defining atoms within molecules. Hence, these quantities are well-defined physical objects integrated over atoms defined in a nonarbitrary way. It is through the analysis of these pair densities that the Lewis model of electronic structure finds physical expression.

The paper is divided into two parts. First we present a detailed analysis of *N*,*N*-dimethylacetamide and the change of the main delocalization indexes as a function of C–N bond rotation. The results for *N*,*N*-dimethylacetamide will be used to set up the conceptual basis for the interpretation of resonance theory in terms of delocalization indexes. In the second part of the paper, the analysis is extended to cover a data set of 24 amides with different degrees of torsion about the C–N bond. It is demonstrated that the use of these indexes is consistent with the traditional view of resonance models in amides. In addition, we show a clear correlation between the delocalization index between nitrogen and oxygen atoms and energetic properties such as the rotational free-energy barrier for these bonds. The proposed index used to characterize the resonance in amides is superior to other correlations based on geometrical parameters such as the torsional angle τ. In addition, it has the conceptual advantage that its physical interpretation is directly linked to electron delocalization arguments through the two-electron pair densities. Thus, we demonstrate that delocalization indexes are reliable quantities to characterize the degree of resonance in amides, and they can be taken as a bridge that reconciles a nonarbitrary partition of the electron density with molecular-orbital-based methods in their interpretation of the resonance model of amides.

Computational Methods

All the geometrical optimizations were carried out in the gas phase using the Gaussian 98 suite of programs[36] at the B3LYP/6-31+G(d) level of theory. The use of the B3LYP functional[37–40] is motivated by its success in the evaluation of reliable reaction enthalpies for the hydrolysis of amides.[41–43] The rotation of *N*,*N*-dimethylacetamide was carried out by constraining the R^1-N-C-O dihedral angle (ω_1 of Figure 1). The τ torsional angle [Eq. (1)] characterizes the mean twisting angle around the C–N bond[44,45] and ranges from 0 (planar amide group) to 90° (when the two planes defined by the O-C-R and R^1-N-R^2 atoms are perpendicular; see Figure 1).

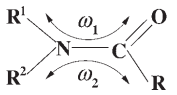

Figure 1. The two dihedral angles (ω_1 and ω_2) used for determining the torsional angle τ. The ω_1 angle was constrained along the *N*,*N*-dimethylacetamide rotation.

$$\tau = \frac{\omega_1 + \omega_2}{2} \quad (1)$$

Moreover, as the rotational free energy of several amides is related to τ and to several delocalization indexes, the struc-

 © 2006 Wiley-VCH Verlag GmbH & Co. KGaA, Weinheim

tures of both the reactants and the rotational transition states were characterized at the B3LYP/6-31+G(d) level of theory. The enthalpic and entropic corrections were determined with frequency calculations at the same level.[46] These frequencies were also used to verify the nature of the stationary points encountered along the potential-energy surfaces. Thus, reactants showed real frequencies for all the normal modes of vibration, whereas rotational transition states showed one imaginary frequency along the normal mode that connects the appropriate minima. The frequency calculations were also used to allow for an evaluation of thermodynamic quantities such as the zero-point vibrational energy, and thermal vibrational contributions to the enthalpy, entropy, and Gibbs free energy.

Insight into the electronic structures of molecules can be gained by using the localization index [Eq. (2)] and the delocalization index [Eq. (3)]:

$$\lambda_A = -\int_A \int_A (2\Gamma(\mathbf{r_1},\mathbf{r_2}) - \rho(\mathbf{r_1})\rho(\mathbf{r_2}))d\mathbf{r_1}d\mathbf{r_2} \quad (2)$$

$$\delta_{AB} = -2\int_A \int_B (2\Gamma(\mathbf{r_1},\mathbf{r_2}) - \rho(\mathbf{r_1})\rho(\mathbf{r_2}))d\mathbf{r_1}d\mathbf{r_2} \quad (3)$$

in which $\rho(\mathbf{r})$ and $\Gamma(\mathbf{r_1},\mathbf{r_2})$ are the one- and two-electron densities, respectively. The delocalization index is formally equivalent to integration of the exchange-correlation density ($\rho_{xc}(\bar{\mathbf{r}}_1,\bar{\mathbf{r}}_2)$) over the basins of atoms A and B (defined from the zero-flux gradient condition applied to the one-electron density, $\rho(\mathbf{r})$), as shown in Equation (4).

$$\delta_{AB} = -2\int_A \int_B \rho_{xc}(\bar{\mathbf{r}}_1,\bar{\mathbf{r}}_2)d\bar{\mathbf{r}}_1 d\bar{\mathbf{r}}_2 \quad (4)$$

The integrations are carried out through one or two atomic basins, as defined from the condition of the zero-flux gradient in $\rho(\mathbf{r})$. Thus, the localization and delocalization indexes are defined in the framework of Bader's theory of Atoms in Molecules (AIM).[27] They were calculated with the AIMPAC suite of programs[47] at the B3LYP/6-31+G(d) level of theory.

The electron-pair density, in conjunction with the definition of an atom in a molecule, enables one to determine the average number of electron pairs that are localized on each atom and that are formed between any given pair of atoms. Localization and delocalization indexes that determine the intra- and interatomic distribution of electron pairs enables one to compare the pairing predicted by theory with that of a Lewis structure. The agreement is best at the Hartree–Fock (HF) level, where the Fermi hole is the sole source of the correlation between electrons. The introduction of the remaining Coulomb correlation disrupts the sharing of electron pairs between the atoms and reduces the number of shared pairs.

The λ and δ indexes are obtained only from first- and second-order densities, which are physical observables. In principle, there is no need to resort to any particular model, such as MO theory, for these calculations. Therefore, provided that ρ and Γ are available, this analysis can be performed at any level of theory. At present, practise provides second-order densities only for the HF and CISD (CISD = configuration interaction for single and double excitations) approximations. In addition, practical quantum calculations are performed in the framework of MO theory. In this case, these indexes can be efficiently calculated through evaluation of the overlap integrals within the corresponding basins. Thus, the delocalization index for a pair of atoms at the HF level of theory would be calculated by using Equation (5):

$$\delta_{AB} = 4\sum_{i,j}^{N/2} S_{ij}(A)S_{ij}(B) \quad (5)$$

The summations run over all the occupied orbitals. The term $S_{ij}(A)$ is the overlap of the orbitals i and j within the basin of atom A.

Within the framework of Kohn–Sham (KS) density functional theory (DFT), $\lambda(A)$ and δ_{AB} cannot be calculated exactly because the electron-pair density has to be approximated by an unknown exchange-correlation functional.[48] As a practical work around, one can derive an HF-like electron-pair density from the KS orbitals and calculate approximate localization and delocalization indexes at the DFT level using Equation (5). Because there is not yet a practical way to obtain molecular electron-pair densities in DFT methods, this is the only feasible approach at the moment for the calculation of approximate delocalization indexes at the DFT level. In fact, although Coulomb correlation effects are included to some extent in the one-electron density, they are not properly taken into account in the two-electron density calculated using the HF ansatz. Therefore, the delocalization indexes obtained using this approximation are generally closer to the HF values than to the correlated ones (e.g., configuration interaction). However, it has been shown that delocalization indexes evaluated within DFT provide useful chemical insight and constitute a suitable tool for the electronic characterization of molecules in different systems, including those with delocalized electrons in aromatic molecules.[49,35,48]

Results and Discussion

Delocalization indexes in *N*,*N*-dimethylacetamide—a case study: We first studied *N*,*N*-dimethylacetamide (Figure 2) as our prototype. The values for the delocalization indexes δ_{CN} and δ_{CO} in *N*,*N*-dimethylacetamide are 1.005 and 1.228 au, respectively. As explained in the Computational Methods section, delocalization indexes at correlated levels of theory tend to give lower values than one would expect from an interpretation of these indexes as the shared electron density in a Lewis model. In order to have some reference values to interpret these indexes as shared electron pairs, we also

 © 2006 Wiley-VCH Verlag GmbH & Co. KGaA, Weinheim

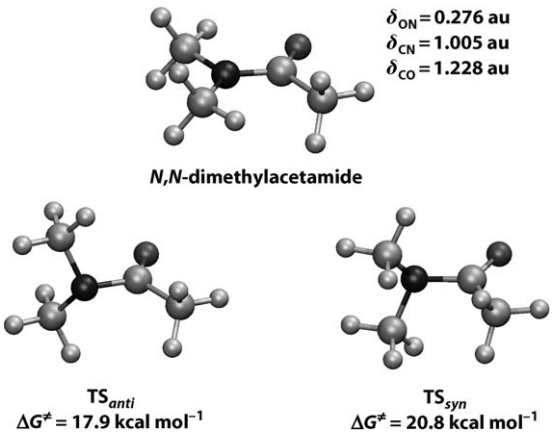

Figure 2. The *N*,*N*-dimethylacetamide reactant and its rotational transition states TS_{anti} and TS_{syn}, which depend on the orientation of n_N with respect to the O atom. Structures were characterized at the B3LYP/6-31+G(d) level of theory.

studied a variety of reference molecules (see Figure 3) at the same level of theory. Molecule $(CH_3)_3C{-}N(CH_3)_2$ was taken as a prototype C–N single bond ($\delta_{CN}=0.915$ au),

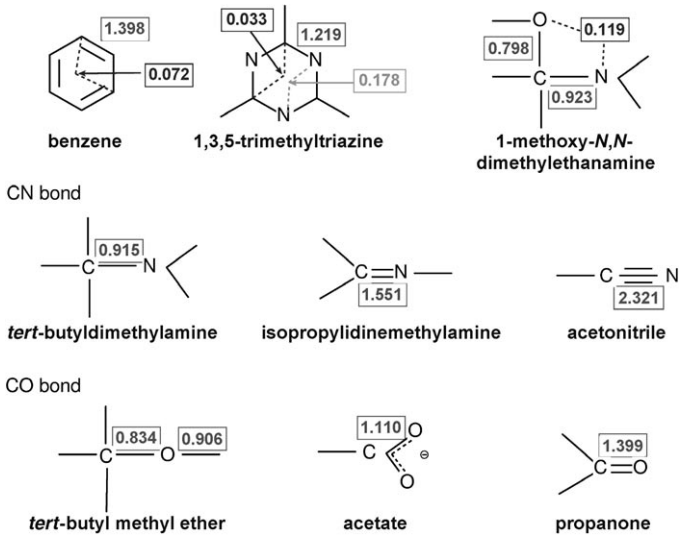

Figure 3. Reference values (in au) for delocalization indexes calculated at the B3LYP/6-31+G(d) level of theory.

$(CH_3)_2C{=}NCH_3$ as a typical C=N double bond ($\delta_{CN}=1.551$ au), and $CH_3C{\equiv}NCH_3$ as a triple C≡N bond ($\delta_{CN}=2.321$ au). Regarding reference indexes for C–O bonds, we considered $(CH_3)_3C{-}OCH_3$ ($\delta_{CO}=0.834$ au) for a single bond, and $(CH_3)_2C{=}O$ for a double bond ($\delta_{CO}=1.399$ au). These indexes are complemented with the values for partial bond orders, such as the one in triazine (C–N bond order of 1.5 and $\delta_{CN}=1.219$ au) and the one in methyl acetate (C–O bond order of 1.5 and $\delta_{CO}=1.110$ au). Notice again that the values for delocalization indexes are significantly lower than the nominal electron pair shared from the Lewis model, as corresponds to the use of correlated level of theory. Based on these reference values, we can asses that the C–N bond in *N*,*N*-dimethylacetamide with $\delta_{CN}=1.005$ au shows a partial double-bond character. Assuming a linear relationship between bond order and δ_{CN} values, an estimation of a bond order of 1.17 was obtained for this bond. Concomitantly, we observed that the C–O bond had partially lost its double-bond character, with $\delta_{CO}=1.228$ au. Assuming again a linear relationship between bond order and δ_{CO}, a bond order of 1.7 was obtained for the C–O bond in *N*,*N*-dimethylacetamide. This is in agreement with the classical resonance model and with the relevance of resonance structures I and II in the description of the electronic structure of amides.

The delocalization indexes are based on the analysis of the second-order electron-density function and provide electron populations that are delocalized between two atoms independent of whether they are directly bound or not. Therefore, we can also measure the delocalization index between nitrogen and oxygen, δ_{ON}. A very high value for this index was observed (0.276 au) even though these two atoms are not directly bound. For instance, in triazine, a lower value for the delocalization between nonbonded nitrogen atoms was obtained (0.178 au). A lower value was also obtained for δ_{ON} (0.119 au) in $CH_3O{-}CH_2{-}N(CH_3)_2$. In the latter, there is no π system in which to delocalize the nitrogen lone pair and, correspondingly, the values of δ_{CO} (0.798 au) and δ_{CN} (0.923 au) suggest single bonds in both cases. The δ_{ON} delocalization index therefore reveals a high electronic delocalization between nitrogen and oxygen. This is consistent with a high delocalization along the N-C-O skeleton, and therefore δ_{ON} could be a good indicator for resonance in amides, although effects such as hyperconjugation and through-space lone-pair interactions could also be contributing to the high δ_{ON} value.

Delocalization indexes and rotation around the C–N bond: Next, we investigated how the delocalization indexes are influenced by C–N bond rotation. Thus, the C-N-C-O dihedral angle was constrained at different values and the delocalization indexes were evaluated. Table 1 shows the electron density and the ellipticity values at the C–N and C–O bond critical points, the torsion angle and the relative energy with respect to the planar *N*,*N*-dimethylacetamide. In Figure 4, the percentage of change in the δ_{CO}, δ_{CN}, and δ_{ON} delocalization indexes as functions of the torsion angle are depicted.

Rotation around the C–N bond can lead to two possible transition states, TS_{anti} and TS_{syn}, with *anti* or *syn* orientation between the oxygen and nitrogen lone pairs (see Figure 4). The free-energy barriers associated with these two transition states are 20.8 kcal mol^{-1} for TS_{syn} and 17.9 kcal mol^{-1} for TS_{anti}. Thus, TS_{anti} is the preferred transition state for rotation, and our choice of dihedral angle for the constrained optimizations leads from the planar *N*,*N*-dimethylacetamide to TS_{anti} (see Table 1). In both transition states, nitrogen adopts a sp^3 hybridization, and therefore, a pyramidal conformation (Figure 4), with concomitant lengthening of the peptide bond and shortening of the carbonyl bond. Rota-

 © 2006 Wiley-VCH Verlag GmbH & Co. KGaA, Weinheim

Table 1. Main parameters along the rotation of *N*,*N*-dimethylacetamide.

ω_1[a]	τ[b]	ΔE[c]	δ_{ON}[d]	δ_{CN}[d]	δ_{CO}[d]	ε_{CN}[e]	ε_{CO}[e]	ρ_{CN}[f]	ρ_{CO}[f]
0.0	0.0	0.0	0.276	1.005	1.228	0.159	0.090	0.314	0.399
8.8	2.6	0.0	0.275	1.004	1.230	0.157	0.090	0.314	0.399
18.9	7.6	0.2	0.273	1.005	1.242	0.151	0.091	0.315	0.399
28.5	13.3	0.8	0.269	1.003	1.245	0.143	0.092	0.315	0.400
37.8	19.5	1.9	0.264	1.001	1.255	0.136	0.092	0.314	0.400
47.0	26.1	3.4	0.256	0.998	1.266	0.129	0.091	0.313	0.401
56.0	33.1	5.4	0.247	0.991	1.279	0.121	0.090	0.310	0.402
66.2	41.3	7.8	0.236	0.981	1.292	0.112	0.088	0.307	0.403
77.3	50.3	10.1	0.222	0.963	1.309	0.100	0.088	0.302	0.405
86.6	58.8	12.4	0.208	0.945	1.324	0.087	0.087	0.297	0.406
96.0	67.9	14.4	0.196	0.925	1.338	0.074	0.085	0.292	0.407
106.4	78.1	15.9	0.187	0.909	1.348	0.063	0.084	0.288	0.408
118.1	90.0	16.4	0.184	0.901	1.351	0.060	0.084	0.287	0.409

[a] The ω_1 dihedral angle was constrained in order to obtain intermediate points along the rotation. [b] Twist angle in degrees. [c] Relative electronic energy in kcal mol^{-1}. [d] Delocalization indexes in au. [e] Ellipticity. [f] Electron density in au.

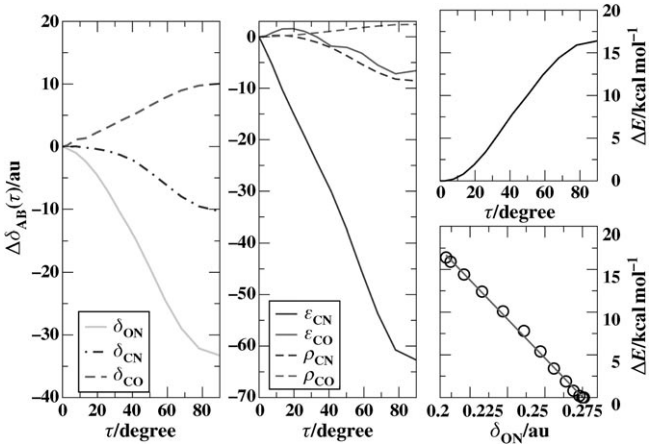

Figure 4. Rotation of *N*,*N*-dimethylacetamide around the C–N bond. Left: the percentage change for δ_{ON}, δ_{CO}, and δ_{CN} indexes with respect to the values in planar *N*,*N*-dimethylacetamide as defined in Equation (6). Center: the percentage change in the C–N and C–O bonds ellipticity and ρ electron density at the bond critical points. Right: the relative electronic energy with respect to the τ torsional angle, and the δ_{ON} index.

Table 2. Electron population (N_A) and localization indexes (λ_A) along the rotation of *N*,*N*-dimethylacetamide towards TS_{anti}.

τ	N_A			λ_A		
	C	N	O	C	N	O
0.0	4.543	8.180	9.217	2.866	6.364	8.299
2.6	4.546	8.176	9.217	2.867	6.380	8.299
7.6	4.561	8.164	9.214	2.874	6.348	8.295
13.3	4.567	8.147	9.211	2.878	6.335	8.292
19.5	4.581	8.127	9.207	2.886	6.318	8.287
26.1	4.596	8.105	9.203	2.895	6.300	8.281
33.1	4.611	8.081	9.199	2.904	6.282	8.276
41.3	4.627	8.059	9.195	2.914	6.266	8.272
50.3	4.643	8.036	9.190	2.926	6.255	8.266
58.8	4.657	8.018	9.184	2.937	6.247	8.260
67.9	4.666	8.006	9.181	2.945	6.245	8.257
78.1	4.673	8.001	9.178	2.953	6.246	8.253
90.0	4.671	8.007	9.177	2.953	6.254	8.253

tional barriers in amides have been extensively studied in the literature.[50–54] The high barriers are attributed to the stabilization caused by the $n_N \rightarrow \pi^*_{CO}$ delocalization, and are therefore a measure of amide bond stability. Wiberg et al. estimated,[55] both theoretically and experimentally, the rotational free-energy barrier in *N*,*N*-dimethylacetamide, and obtained a barrier of 15.3 ± 0.1 kcal mol^{-1} experimentally (with respect to TS_{anti}) using NMR selective inversion–recovery experiments in several solvents. They also calculated the barrier by using quantum methods (at the G2(MP2) level of theory), giving a value of 15.64 kcal mol^{-1} for TS_{anti} and 18.13 kcal mol^{-1} for TS_{syn} in good agreement with experiments and with our own results.

Variations of δ_{CN}, δ_{CO}, and δ_{ON} delocalization indexes as functions of the C–N bond rotation are shown in Table 1. In Figure 4, the percentage change in localization indexes [$\Delta\delta_{AB}(\tau)$; Eq. (6)] with respect to the values at the planar amide are depicted:

$$\Delta\delta_{AB}(\tau) = \frac{\delta_{AB}(\tau) - \delta_{AB}(\tau = 0.0)}{\delta_{AB}(\tau = 0.0)} \times 100 \qquad (6)$$

The value of δ_{CO} increases from 1.228 au in planar *N*,*N*-dimethylacetamide to 1.351 au in TS_{anti}, whereas δ_{CN} decreases from 1.005 au in planar *N*,*N*-dimethylacetamide to 0.901 au in TS_{anti}. At the transition state, the values of δ_{CN} and δ_{CO} are indicative of the presence of a C–N single bond and a C=O double bond, in agreement with the resonance model, which would predict a loss in the contribution of resonant structure II upon rotation. The δ_{ON} index, shown in Figure 4, is extremely sensitive to C–N bond rotation. It goes from 0.276 au in planar *N*,*N*-dimethylacetamide to 0.184 au in TS_{anti}. This value still shows some degree of delocalization between the nitrogen and oxygen atoms, although the analysis of δ_{CN} and δ_{CO} prevents the association of this delocalization to a π-type delocalized interaction.

The changes in electron delocalization indexes are also reflected to a certain extent by the change in properties at the bond critical points. The density at the C–N bond critical point lowers (from 0.314 to 0.287 au) and the one at the C–O bond slightly increases (from 0.399 to 0.409 au). However, the analysis of the values of the ellipticities (which measures the anisotropy of the curvature of the electron density)[56] at these critical points leads to contradictory results for the C–O bond. The value of ε_{CN} shows a dramatic decrease of 70% in accordance with a loss in C–N double-bond character. However, ε_{CO} also shows a decrease of approximately 5%, which is in disagreement with a reinforcement of the π character of the bond. This result pinpoints the limitations of the use of analyses based on the properties of just one point in space. Delocalization indexes are integrated in volumes of well-defined boundaries and are, in this sense, taking into account the whole atomic volume.

Analysis of the localization indexes and atomic charges (see Table 2) lead to similar results as those described by Wiberg et al.,[21,22] namely an increase in electronic charge on the carbon atom and a decrease on the nitrogen atom.

 © 2006 Wiley-VCH Verlag GmbH & Co. KGaA, Weinheim

The electronic charge associated with the oxygen atom decreases upon rotation but to a much lesser degree. This behavior, which is somewhat contrary to that predicted by the traditional resonance model, has generated an interesting theoretical discussion on the origin of amide stabilization. The interpretation associated with Bader atomic charges is still a matter of controversy. In addition, several experimental estimates of trends of atomic charges upon rotation suggest that Bader atomic charges give the wrong trend. For instance, Yamada[28] characterized, by X-ray diffraction, the structure of 3-acyl-1,3-thiazolidine-2-thione derivatives and related their τ torsional angle to the ^{13}C, ^{15}N, and ^{17}O NMR chemical shifts. The results showed that as the twist angle increases, $\Delta\delta^{13}C$ and $\Delta\delta^{17}O$ increase while $\Delta\delta^{15}N$ decreases. These $\Delta\delta$ chemical shifts are directly related to the charge densities around each atom. Therefore, the increment of the twist of the amide bond leads to a decrease in the electron density of the C and O atoms and an increase in that of the N atom, in agreement with what the resonance model would predict. Greenberg et al.[29] reached similar conclusions based on the analysis of the N1s and O1s core ionization energies for a group of planar and distorted amides and lactams by using X-ray photoelectron spectroscopy. On the other hand, when the analysis of the electron density in these compounds is carried out in terms of electron-pair densities integrated in the corresponding atomic basins rather than in terms of atomic-charge densities, the discrepancies with the resonance model disappear.

In summary, the trend of the delocalization indexes supports the traditional resonance model in that a decrease in the electron sharing between the carbon and nitrogen atoms and an increase between the carbon and oxygen atoms is observed with C–N bond rotation. Moreover, there is a high electron delocalization between the nitrogen and oxygen atoms, only possible if there is substantial electronic resonance along the N-C-O skeleton. In this sense, rotation around the C–N bond leads to a substantial decrease in δ_{ON}. In addition, when the values of this index are plotted versus the relative energies of the structures with different degrees of twisted amide bond (Figure 4, right-bottom diagram), there is a clear correlation ($r=-0.9990$) between decrease in δ_{ON} and energetic destabilization of the structure. Its physical interpretation is consistent with the classical resonance model. Thus, it seems that δ_{ON} is an ideal physical-chemical property to measure the degree of electronic delocalization along the N-C-O skeleton in amides. To investigate this hypothesis, a more general analysis was required with a sufficiently large amide data set. This is the subject of the next section.

Delocalization indexes in an amide data set: A series of 24 amides with varying degree of twist were investigated (Figure 5). Amides were classified in three different families depending on the functional group attached to the carbonyl carbon (R in Figure 5): a hydrogen atom or a methyl or phenyl group. To provoke different torsions on the amide bond, different substituents were attached to the nitrogen

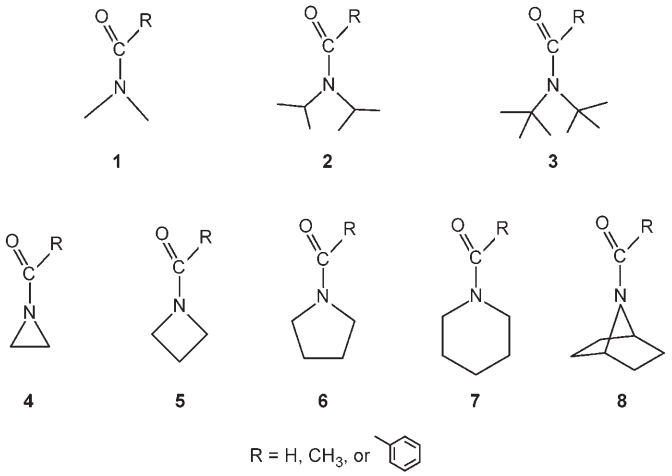

Figure 5. Amide data set studied at the B3LYP/6-31+G(d) level of theory. Three different families were characterized depending on the group attached to the carbonyl group (R = H, methyl, or phenyl). Notice that compounds **1**–**3** are aliphatic while **4**–**8** are cyclic amides for which the degree of N pyramidalization, and therefore the τ twist angle, changes. The TS_{anti} structures were also characterized at the same level of theory in order to determine the corresponding rotational free-energy barrier.

atom. In compound **1** we introduced two methyl groups, in **2**, two isopropyl groups, and in **3**, two *tert*-butyl groups. In addition, the nitrogen atom was embedded in a ring whose size and, hence, the level of amide bond twist, was varied from compounds **4** to **8**. To facilitate the identification of these amides, a number code was employed (illustrated in Figure 5) with a subscript defining the substituent (R) at the carbon position: H (H), methyl (Met), or phenyl (Phe). We first discuss the selected geometrical features of the characterized structures, and then their rotational free-energy barriers and delocalization indexes.

Geometries: The main geometrical parameters for the reactants and TS_{anti} transition states are presented in Table 3. The different substituents have a large effect on the degree of amide bond torsion. For instance, dimethylformamide ($\mathbf{1_H}$) is completely planar ($\tau=0.0°$), but as more-bulky substituents are added at the nitrogen position, the planarity is broken, and compound $\mathbf{3_H}$ has $\tau=7.5°$. Substitution at the R position also leads to sizeable differences in the degree of amide bond torsion, especially when phenyl groups are introduced. For example, while compounds $\mathbf{1_H}$ and $\mathbf{1_{Met}}$ are planar, compound $\mathbf{1_{Phe}}$ is significantly twisted with $\tau=13.9°$. In general, we observed that the planarity of the compounds decreased as we went from R = H to Met, and from R = Met to Phe, with the average τ angle over the eight compounds being 2.8° for R = H, 9.3° for R = Met, and 18.4° for R = Phe. With respect to substitution at the nitrogen atom, the greatest degree of twist was obtained for compounds of **3**, with a bulky *tert*-butyl substituent, and **4**, which has the smallest ring structure and therefore a very constrained environment around the nitrogen atom. As we added less-bulky substituents (compounds **1** or **2**), or as the size of the

 © 2006 Wiley-VCH Verlag GmbH & Co. KGaA, Weinheim

Table 3. Torsional angle (in degrees) and CN and CO bond lengths (in Å), for compounds **1**–**8** and their corresponding rotational transition states.

Molecule	R = H			R = Methyl			R = Phenyl		
	τ	r_{CN}	r_{CO}	τ	r_{CN}	r_{CO}	τ	r_{CN}	r_{CO}
1	0.0	1.364	1.224	0.0	1.375	1.231	13.9	1.376	1.233
TS$_1$	90.0	1.440	1.209	90.0	1.456	1.214	90.0	1.452	1.220
2	0.2	1.368	1.226	2.9	1.381	1.234	16.0	1.378	1.236
TS$_2$	89.5	1.428	1.213	86.2	1.445	1.217	84.4	1.440	1.223
3	7.5	1.374	1.230	43.7	1.400	1.228	49.5	1.407	1.230
TS$_3$	89.2	1.435	1.212	88.1	1.453	1.217			
4	11.1	1.384	1.216	17.9	1.398	1.221	21.4	1.402	1.224
TS$_4$	90.0	1.426	1.212	90.0	1.442	1.216	90.0	1.439	1.222
5	0.0	1.349	1.227	1.5	1.359	1.232	10.0	1.368	1.234
TS$_5$	90.0	1.432	1.211	90.0	1.447	1.216	90.0	1.444	1.222
6	0.2	1.353	1.227	0.8	1.364	1.233	8.1	1.367	1.236
TS$_6$	90.0	1.435	1.211	90.0	1.450	1.215	90.0	1.446	1.221
7	0.1	1.358	1.227	2.4	1.371	1.233	11.4	1.371	1.235
TS$_7$	90.0	1.433	1.210	90.0	1.449	1.215	89.8	1.445	1.221
8	3.1	1.356	1.226	5.3	1.370	1.231	16.5	1.376	1.233
TS$_8$	90.0	1.430	1.213	90.0	1.444	1.217	90.0	1.439	1.223

ring was increased (compounds **5**, **6**, or **7**), the amides became more planar. Similar effects introduced by bulky substituents[57] and with differing ring sizes[58] have been reported in the literature.

Rotational transition states: Rotational transition states for each of the 24 amides of the series were also characterized (see Table 4), except in the case of **3$_{Phe}$** for which all attempts to trap the transition state failed. All transition states display torsional τ angles close to 90.0°. The trends in C–N and C–O bond lengths are the same for all systems, in that torsion around the C–N bond leads to an elongation of the C–N bond and a reduction of the C–O bond. Rotational free-energy barriers show large variations, from 3.4 kcal mol^{-1} for **1$_{Met}$** to 23.4 kcal mol^{-1} for **7$_H$**. These variations reveal substantial differences in the stability of the amides, and have their formal origin in the differences in electron resonance caused by the specific degree of torsion induced in each amide. The relationship between geometrical parameters and amide bond stability is well established. For instance, Brown et al.[59] showed a relationship between the distortion of the amide bond and the rate of hydrolysis in both acid and base. In general, the more twisted the amide bond the lower the rotational barrier and, therefore, the weaker the C–N bond. Figure 6 shows the values of the free-energy barriers versus the degree of amide bond twist (τ angle) of the amide reactant. There is an inverse relationship between these two properties with a correlation coefficient of −0.8550. Brown and co-workers related the amide carbonyl stretching frequencies to the rotational barrier for a set of anilides and toluamides.[60] Moreover, they correlated the rotational barrier with the C–N amide bond length indicating that short amide bond lengths yielded higher rotational barriers. On plotting our calculated barriers versus the C–N bond lengths (Figure 6), we also found a linear inverse relation ($r = -0.905$).

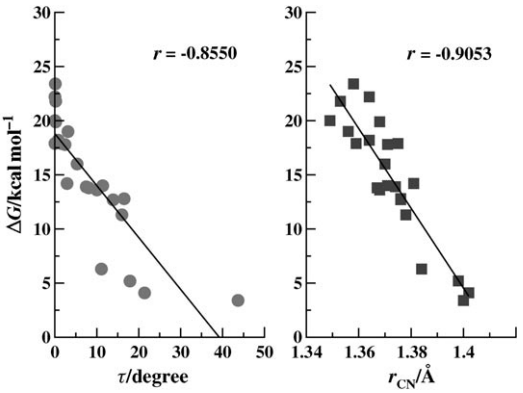

Figure 6. Representation of the rotational energy of different twisted amides with respect to the torsional angle (left) and the C–N bond length (right). The correlation coefficients among the points of each graphic are shown.

Table 4. Rotational free energies (ΔG_{rot} in kcal mol^{-1}), and O-N, C-N, and C-O delocalization indexes (in au) for compounds **1**–**8** and their rotational transition states.

Molecule	R = H				R = Methyl				R = Phenyl			
	ΔG_{rot}	δ_{ON}	δ_{CN}	δ_{CO}	ΔG_{rot}	δ_{ON}	δ_{CN}	δ_{CO}	ΔG_{rot}	δ_{ON}	δ_{CN}	δ_{CO}
1	22.2	0.288	1.026	1.269	17.9	0.276	1.005	1.228	12.7	0.274	1.007	1.225
TS$_1$		0.190	0.929	1.410		0.182	0.897	1.347		0.179	0.901	1.317
2	19.9	0.280	1.046	1.265	14.2	0.268	1.031	1.225	11.3	0.270	1.032	1.226
TS$_2$		0.192	0.934	1.396		0.185	0.908	1.339		0.182	0.913	1.307
3	13.9	0.272	1.052	1.259	3.4	0.246	1.000	1.251		0.232	0.991	1.251
TS$_3$		0.185	0.931	1.375		0.179	0.905	1.324				
4	6.3	0.266	0.982	1.327	5.2	0.250	0.954	1.284	4.1	0.239	0.950	1.268
TS$_4$		0.203	0.962	1.374		0.193	0.925	1.319		0.190	0.926	1.292
5	20.0	0.300	1.023	1.265	17.9	0.287	0.991	1.224	13.6	0.277	0.997	1.221
TS$_5$		0.193	0.947	1.401		0.185	0.913	1.338		0.181	0.917	1.309
6	21.8	0.295	1.027	1.263	18.2	0.282	1.001	1.221	13.8	0.279	1.009	1.214
TS$_6$		0.190	0.936	1.404		0.182	0.904	1.342		0.179	0.907	1.312
7	23.4	0.291	1.033	1.261	17.8	0.278	1.013	1.222	14.0	0.276	1.017	1.217
TS$_7$		0.190	0.934	1.403		0.182	0.902	1.342		0.179	0.905	1.312
8	19.0	0.292	1.021	1.271	16.0	0.277	0.993	1.234	12.8	0.267	0.996	1.231
TS$_8$		0.189	0.949	1.397		0.181	0.915	1.337		0.178	0.918	1.307

Delocalization indexes: Delocalization indexes are given in Table 4. Comparison of the data for each amide with its transition state is consistent with the predictions of the resonance model: a lowering of the electron sharing between the carbon and nitrogen atoms and an increase in the electron sharing between the carbon and oxygen atoms, or in other words: 1) a lowering of δ_{CN} towards values typical of C–N single bonds, and 2) an increase in δ_{CO} to values closer to those of C–O double bonds.

 © 2006 Wiley-VCH Verlag GmbH & Co. KGaA, Weinheim

Changes in δ_{ON} are also consistent with these electronic changes, and at any of the transition states, the values for δ_{ON} are significantly lower than those of the amide reactant. However, the specific values for δ_{ON} vary significantly among the various compounds. From 0.300 au for $\mathbf{4_H}$ to 0.232 au for $\mathbf{3_{Phe}}$. In general, compounds with R = H have the largest values for δ_{ON}, with an average δ_{ON} of 0.286 au calculated among the eight amide reactants, compared with R = Met with average $\delta_{ON} = 0.271$ au, and finally, the lowest values are found for the R = Phe series, with an average of 0.264 au. This indicates a substantial π-electron-withdrawing effect by the phenyl group. In addition, there is a direct correlation between the degree of N–O delocalization and rotational barrier. Thus, in Figure 7, we plotted the values of

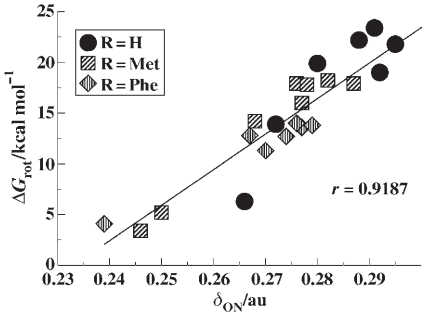

Figure 7. Rotational free energy versus δ_{ON} delocalization index for the amide data set.

δ_{ON} versus the rotational barriers. A linear correlation was obtained ($r = 0.9187$), indicating the direct relation between high electron delocalization between nitrogen and oxygen basins and the stability of the amide bond as characterized by values of the rotational barriers. The advantage of using δ_{ON} for this type of correlation is that this parameter is sensitive not only to geometrical changes in amides but also to electronic effects induced by the different substituents, which could not be directly inferred from changes in the degree of planarity of the amide. For example, both $\mathbf{1_H}$ and $\mathbf{1_{Met}}$ are planar (τ is 0.0°), but the rotational barrier is 22.2 kcal mol^{-1} for the former and 17.9 kcal mol^{-1} for the latter, indicating that the electron delocalization and its induced stabilization should be stronger in $\mathbf{1_H}$. An analysis of δ_{ON} effectively reproduced a change in the degree of electron delocalization in these two amides, and $\mathbf{1_H}$ shows a higher value for the delocalization index (0.288 au, compared with $\delta_{ON}(\mathbf{1_{Met}}) = 0.276$ au). The linear fit can also be done for each set of compounds, obtaining the following correlation coefficients: $r = 0.8270$ (R = H); $r = 0.9733$ (R = Me); $r = 0.9762$ (R = Phe). Thus, notice the worst linear fit is obtained for compounds with R = H, which could be due to internal hydrogen-bonding interactions affecting the values of rotational free-energy barriers and that are not directly characterized by delocalization indexes.

Attempts to correlate rotational barriers and parameters derived from electronic structure calculations are not new. For instance, Otani et al.[58] found a good correlation between the experimental rotational free-energy barrier in solution of a series of *N*-benzoyl-7-azabicyclo[2.2.1]heptanes with respect to the delocalization indexes derived from differences in the relative ratio of the coefficients for the n_N orbital and the π^*_{CO} orbital between the transition state and the ground state configuration. However, the use of indexes such as δ_{ON} to characterize electron delocalization has the appeal of being a well-defined quantum mechanical quantity, being in principle less dependent on the choice of molecular orbitals, and not relying on an arbitrary partitioning of the electron density. However, it should also be remarked that, in practise, the use of an approximate density functional and limited basis set puts a limitation on the degree of accuracy of the present calculations.

Relation between delocalization indexes and geometrical parameters: The relation between delocalization indexes and selected interatomic distances (r_{ON}, r_{CN}, and r_{CO}) was also investigated. For the relaxed amide structures, the following trends were found (Figure 8): 1) there is a linear relationship between δ_{ON} and r_{CN}, but the correlation of δ_{ON} with r_{CO} and r_{ON} is less clear; 2) r_{CO} correlates well with δ_{CO}; 3) poor correlation between δ_{CN} and r_{CN}.

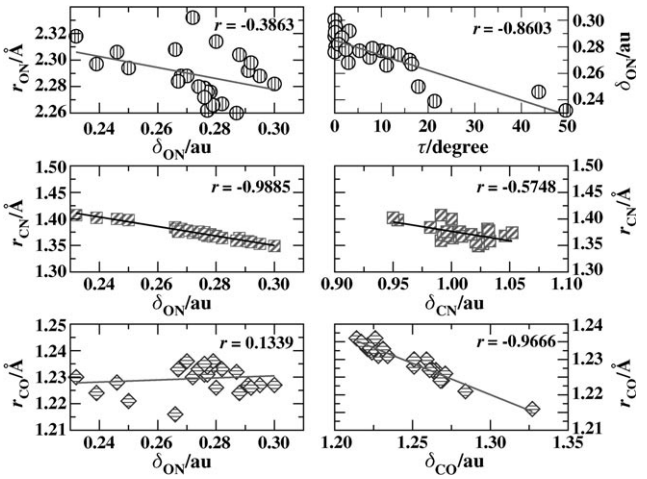

Figure 8. Relation between the delocalization indexes and geometrical parameters of the amide reactants.

At the transition states (Figure 9), there are changes in these trends: 1) no clear correlation between δ_{ON} and any of the r_{ON}, r_{CN}, or r_{CO} distances; 2) clear inverse relations between δ_{CO} and r_{CO}, and between δ_{CN} and r_{CN}.

These results suggest that in amides the r_{CN} bond length is most sensitive to the degree of delocalization between the nitrogen and oxygen atoms, and differences in this distance can efficiently monitor changes in resonance along the N-C-O skeleton. This result supports the use of the r_{CN} geometrical parameter to provide a quantitative estimate of the degree of electron resonance in amides as suggested by

 © 2006 Wiley-VCH Verlag GmbH & Co. KGaA, Weinheim

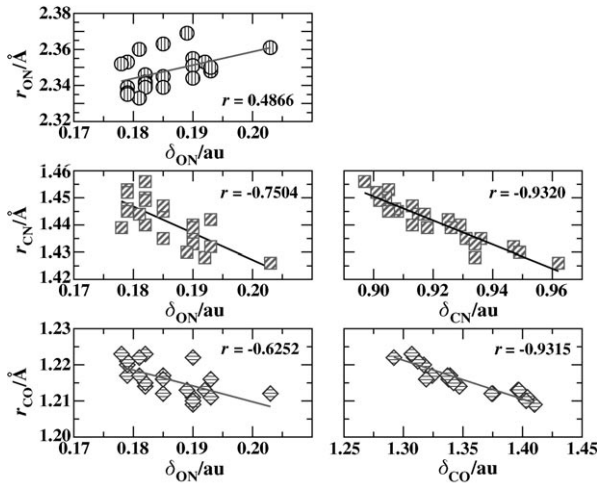

Figure 9. Relation between the delocalization indexes and geometrical parameters of the transition states.

Brown et al.[60] Furthermore, Laidig and Cameron[26] pointed out that the predominant change upon pyramidalization of N is the weakening of the C–N interaction. On the contrary, we find that C–O bond lengths are quite insensitive to the degree of δ_{NO} delocalization, which could explain why there is little change in this distance upon C–N bond rotation. Interestingly, at the transition-state structures, in which the possibility of π-type resonance is disrupted, both C–N and C–O bonds are linearly correlated to their own interatomic delocalization indexes (δ_{CN} and δ_{CO}, respectively).

Regarding the torsional angle, τ, the best correlation is obtained to the delocalization index δ_{ON}. However, this is significantly poorer than the one obtained between δ_{ON} and r_{CN} and, therefore, it seems that τ is a less efficient geometrical parameter for the characterization of electron resonance.

Conclusions

Electron resonance is an important concept to rationalize the special geometrical and energetic features of amides. However, there is not a unique way to measure the degree of electron resonance or delocalization in a given chemical structure. In the present paper, we have shown how electron resonance in amides can be characterized in terms of quantities derived from the two-electron density matrix and integration over atomic basins derived from the zero-flux surface condition. The physical interpretation of pair densities as simultaneous probability densities of finding electrons at two points in space allows for a direct connection of these quantities with chemical concepts such as resonance or delocalization. In particular, we have demonstrated that the delocalization index between nitrogen and oxygen atoms (δ_{ON}) is a reliable tool to analyze the electron delocalization through the N-C-O skeleton in amides. Our results suggest a linear relationship between this delocalization index and the rigidity of the amide bond, inferred through the values of its rotational barriers. In addition, the use of this index gives a picture for the electron resonance in amides very close to the traditional resonance model, and could overcome the discrepancies found between these models and previous applications of Bader-type analyses.

Acknowledgements

This research was funded by Euskal Herriko Unibertsitatea (the University of the Basque Country), Gipuzkoako Foru Aldundia (the Provincial Government of Gipuzkoa), Eusko Jaurlaritza (the Basque Government), and the Swedish Science Research Council (UR). J.I.M. thanks the University of the Basque Country for a predoctoral grant. We are grateful to Dr. Jordi Poater (Universitat de Girona) for useful discussions and technical help in doing the calculations of the localization and delocalization indexes. The SGI/IZO-SGIker UPV/EHU (supported by Fondo Social Europeo and M.C.yT.) is gratefully acknowledged for generous allocation of computational resources.

[1] A. L. Lehninger, D. L. Nelson, M. M. Cox, *Principles of Biochemistry*, Worth, New York, **1993**.
[2] "Studies in Amide Hydrolysis: The Acid, Base, and Water Reactions": R. S. Brown in *The Amide Linkage: Structural Significance in Chemistry, Biochemistry, and Materials Science* (Eds.: A. Greenberg, C. M. Breneman, J. F. Liebman) Wiley, New York, **2000**.
[3] P. Chakrabarti, J. D. Dunitz, *Helv. Chim. Acta* **1982**, *65*, 1555–1562.
[4] E. Hirota, R. Sugisaki, C. J. Nielsen, G. O. Sørensen, *J. Mol. Spectrosc.* **1974**, *49*, 251–267.
[5] K. Vankatesan, S. Ramakumar, *Structural Studies of Molecular Biological Interest*, Oxford University, Oxford, UK, **1981**, pp. 137–153.
[6] B. Sunners, L. H. Piette, W. G. Schneider, *Can. J. Chem.* **1960**, *38*, 681–688.
[7] T. Drakenberg, S. Forsen, *J. Phys. Chem.* **1970**, *74*, 1–7.
[8] M. B. Robin, F. A. Bovey, H. Basch, *The Chemistry of Amides*, Wiley-Interscience, London, **1970**, pp. 1–72.
[9] W. E. Stewart, T. H. Siddall, *Chem. Rev.* **1970**, *70*, 517–551.
[10] Y. Toriumi, A. Kasuya, A. Itai, *J. Org. Chem.* **1990**, *55*, 259–263.
[11] J. Hine, R. S. M. King, W. R. Midden, A. Sinha, *J. Org. Chem.* **1981**, *46*, 3186–3189.
[12] A. Radzicka, R. Wolfenden, *J. Am. Chem. Soc.* **1996**, *118*, 6105–6109.
[13] L. Pauling, *The Nature of the Chemical Bond*, 3rd ed., Cornell University Press, Ithaca, New York, **1960**.
[14] L. Pauling, G. W. Wheland, *J. Chem. Phys.* **1933**, *1*, 362–374.
[15] G. W. Wheland, L. Pauling, *J. Am. Chem. Soc.* **1935**, *57*, 2086–2095.
[16] G. W. Wheland, *The Theory of Resonance and Its Applications to Organic Chemistry*, Wiley, New York, **1955**.
[17] E. D. Glendening, J. A. Hrabal II, *J. Am. Chem. Soc.* **1997**, *119*, 12940–12946.
[18] C. Fogarasi, P. Szalay, *J. Phys. Chem. A* **1997**, *101*, 1400–1408.
[19] D. Lauvergnat, P. Hiberty, *J. Am. Chem. Soc.* **1997**, *119*, 9478–9482.
[20] Y. Mo, P. von R. Schleyer, W. Wu, M. Lin, Q. Zhang, J. Gao, *J. Phys. Chem. A* **2003**, *107*, 10011–10018.
[21] K. B. Wiberg, K. E. Laidig, *J. Am. Chem. Soc.* **1987**, *109*, 5935–5943.
[22] K. B. Wiberg, C. M. Breneman, *J. Am. Chem. Soc.* **1992**, *114*, 831–840.
[23] K. B. Wiberg, C. M. Hadad, P. R. Rablen, J. Cioslowski, *J. Am. Chem. Soc.* **1992**, *114*, 8644–8654.
[24] K. B. Wiberg, P. R. Rablen, *J. Am. Chem. Soc.* **1993**, *115*, 9234–9242.
[25] K. B. Wiberg, P. R. Rablen, *J. Am. Chem. Soc.* **1995**, *117*, 2201–2209.
[26] K. E. Laidig, L. M. Cameron, *J. Am. Chem. Soc.* **1996**, *118*, 1737–1742.

 © 2006 Wiley-VCH Verlag GmbH & Co. KGaA, Weinheim

[27] R. F. W. Bader, *Atoms in Molecules: A Quantum Theory*, Clarendon Press, Oxford, UK, **1990**.
[28] S. Yamada, *J. Org. Chem.* **1996**, *61*, 941–946.
[29] A. Greenberg, T. D. Thomas, C. R. Bevilacqua, M. Coville, D. Ji, J. C. Tsai, G. Wu, *J. Org. Chem.* **1992**, *57*, 7093–7099.
[30] K. B. Wiberg, D. J. Rush, *J. Am. Chem. Soc.* **2001**, *123*, 2038–2046.
[31] C. L. Perrin, *J. Am. Chem. Soc.* **1991**, *113*, 2865–2868.
[32] K. E. Laidig, *J. Am. Chem. Soc.* **1992**, *114*, 7912–7913.
[33] C. Gatti, P. Fantucci, *J. Phys. Chem.* **1993**, *97*, 11677–11680.
[34] X. Fradera, M. A. Austen, F. W. Bader, *J. Phys. Chem. A* **1999**, *103*, 304–314.
[35] J. Poater, M. Solà, M. Duran, X. Fradera, *J. Phys. Chem. A* **2001**, *105*, 2052–2063.
[36] Gaussian 98 (Revision A.2), M. J. Frisch, G. W. Trucks, H. B. Schlegel, G. E. Scuseria, M. A. Robb, J. R. Cheeseman, V. G. Zakrzewski, J. A. Montgomery, Jr., R. E. Stratmann, J. C. Burant, S. Dapprich, J. M. Millam, A. D. Daniels, K. N. Kudin, M. C. Strain, O. Farkas, J. Tomasi, V. Barone, M. Cossi, R. Cammi, B. Mennucci, C. Pomelli, C. Adamo, S. Clifford, J. Ochterski, G. A. Petersson, P. Y. Ayala, Q. Cui, K. Morokuma, D. K. Malick, A. D. Rabuck, K. Raghavachari, J. B. Foresman, J. Cioslowski, J. V. Ortiz, B. B. Stefanov, G. Liu, A. Liashenko, P. Piskorz, I. Komaromi, R. Gomperts, R. L. Martin, D. J. Fox, T. Keith, M. A. Al-Laham, C. Y. Peng, A. Nanayakkara, C. Gonzalez, M. Challacombe, P. M. W. Gill, B. G. Johnson, W. Chen, M. W. Wong, J. L. Andres, M. Head-Gordon, E. S. Replogle, J. A. Pople, Gaussian, Inc., Pittsburgh, PA, **1998**.
[37] S. H. Vosko, L. Wilk, M. Nusair, *Can. J. Phys.* **1980**, *58*, 1200–1211.
[38] A. Becke, *Phys. Rev. A* **1988**, *38*, 3098–3100.
[39] C. Lee, W. Yang, R. Parr, *Phys. Rev. B* **1988**, *37*, 785–789.
[40] A. Becke, *J. Chem. Phys.* **1993**, *98*, 5648–5652.
[41] K. D. Dobbs, D. A. Dixon, *J. Phys. Chem.* **1996**, *100*, 3965–3973.
[42] X. Lopez, J. Mujika, G. Blackburn, M. Karplus, *J. Phys. Chem. A* **2003**, *107*, 2304–2315.
[43] J. I. Mujika, J. M. Mercero, X. Lopez, *J. Am. Chem. Soc.* **2005**, *127*, 4445–4453.
[44] G. Gilli, V. Bertolasi, F. Belluccu, V. Ferretti, *J. Am. Chem. Soc.* **1986**, *108*, 2420–2424.
[45] V. Ferretti, V. Bertolasi, P. Gilli, G. Gilli, *J. Phys. Chem.* **1993**, *97*, 13568–13574.
[46] W. Hehre, L. Radom, P. von R. Schleyer, J. Pople, *Ab Initio Molecular Orbital Theory*, Wiley-Interscience, New York, **1986**.
[47] F. W. Biegler-König, R. F. W. Bader, T. H. Tang, *J. Comput. Chem.* **1982**, *3*, 317–328.
[48] J. Poater, M. Solà, M. Duran, X. Fradera, *Theor. Chem. Acc.* **2002**, *107*, 362–371.
[49] T. M. Krygowski, K. Ejsmont, B. T. Stepien, M. K. Cyranski, J. Poater, M. Solà, *J. Org. Chem.* **2004**, *69*, 6634–6640.
[50] L. F. Olson, Y. Li, K. N. Houk, A. J. Kresge, L. J. Schaad, *J. Am. Chem. Soc.* **1995**, *117*, 2992–2997.
[51] R. F. Nalewajski, *J. Am. Chem. Soc.* **1978**, *100*, 41–46.
[52] J. O. Williams, C. van Alsenoy, L. Schafer, *THEOCHEM* **1981**, *76*, 171–177.
[53] P. G. Jasien, W. J. Stevens, M. Krauss, *THEOCHEM* **1986**, *139*, 197–206.
[54] S. Tsuzuki, K. Tanabe, *J. Chem. Soc. Perkin Trans. 2* **1991**, *8*, 1255–1960.
[55] K. B. Wiberg, P. R. Rablen, D. J. Rusch, T. A. Keith, *J. Am. Chem. Soc.* **1995**, *117*, 4261–4270.
[56] C. Silva, O. Nieto, F. Cossio, D. York, A. de Lera, *Chem. Eur. J.* **2005**, *11*, 1734–1738.
[57] Y. Jean, I. Demachy, A. Lledos, F. Maseras, *THEOCHEM* **2003**, *632*, 131–144.
[58] Y. Otani, O. Nagae, Y. Naruse, S. Inagaki, M. Ohno, K. Yamaguchi, G. Yamamoto, M. Uchiyama, T. Ohwada, *J. Am. Chem. Soc.* **2003**, *125*, 15191–15199.
[59] Q. P. Wang, A. J. Bennet, R. S. Brown, B. D. Santarsiero, *J. Am. Chem. Soc.* **1991**, *113*, 5757–5765.
[60] A. J. Bennet, V. Somayaji, R. S. Brown, B. D. Santarsiero, *J. Am. Chem. Soc.* **1991**, *113*, 7563–7571.

Received: January 13, 2006
Published online: June 28, 2006

 © 2006 Wiley-VCH Verlag GmbH & Co. KGaA, Weinheim